

SPATIAL INTERPOLATION OF RAINFALL INTENSITY IN JAVA ISLAND USING ORDINARY KRIGING

**Shabira A. Auliyazhafira¹, Fariza A. Putri², Theresia S. Nauli³, Aulia R. Al Madani⁴,
I Gede Nyoman Mindra Jaya⁵, Annisa N. Falah⁶, Budi Nurani Ruchjana^{7*}**

^{1,2,3,4}Master's Program in Applied Statistics, Department of Statistics, Faculty of Mathematics and
Natural Sciences, Universitas Padjadjaran

⁵Department of Statistics, Faculty of Mathematics and Natural Sciences, Universitas Padjadjaran

^{6,7}Department of Mathematics, Faculty of Mathematics and Natural Sciences, Universitas Padjadjaran
Jl. Ir. Soekarno km 21 Jatinangor, Sumedang, 45363, Indonesia

Corresponding author's e-mail: * budi.nurani@unpad.ac.id

ABSTRACT

Article History:

Received: 21st October 2024

Revised: 6th February 2025

Accepted: 4th April 2025

Published: 1st July 2025

Keywords:

MAPE;

Ordinary Point Kriging;

Power NASA;

Rainfall;

Semivariogram.

Indonesia, situated between two continents and two oceans, experiences a complex climate system influenced by global warming. Climate change has disrupted weather patterns, making it increasingly difficult to predict the rainy and dry seasons and rainfall intensity. However, neighboring regions often exhibit similar weather characteristics, which can be leveraged for prediction. As Indonesia's economic center, Java Island displays distinct yet interconnected weather patterns, making accurate rainfall prediction crucial for various sectors. This study utilizes 10 years of average rainfall data from NASA's Power database, covering 64 observation points across Java. Ordinary point kriging is the estimation of a value at a given point and is often used in spatial interpolation analysis in general. Through ordinary point kriging analysis, this study aims to find an accurate kriging equation for predicting rainfall in various regions of Java Island. To achieve this, semivariogram modeling was performed to determine the best theoretical model for spatial interpolation. From 53 sampled regions, 1,378 sample pairs were used to calculate the experimental semivariogram obtained using the R programming language. Next, the theoretical semivariogram was determined using the sill parameter derived from the variance of the sampled data. Three theoretical semivariogram models were considered: spherical, exponential, and Gaussian. The results indicated that the exponential model was the most suitable as it had the smallest SSE value. The results of this analysis enrich our understanding of climate patterns in Indonesia and will contribute to developing mitigation and adaptation strategies related to climate change in the future. The Kriging equation obtained can provide highly accurate prediction results on the test data with a MAPE (Mean Absolute Percentage Error) error measure of 4.85% and RMSE (Root Mean Square Error) of 18.17, which indicates that the prediction results obtained are highly accurate predictions.



This article is an open access article distributed under the terms and conditions of the [Creative Commons Attribution-ShareAlike 4.0 International License](https://creativecommons.org/licenses/by-sa/4.0/).

How to cite this article:

S. A. Auliyazhafira, F. A. Putri, T. S. Nauli, A. R. A. Madani, I. G. N. M. Jaya, A. N. Falah, B. N. Ruchjana., "SPATIAL INTERPOLATION OF RAINFALL INTENSITY IN JAVA ISLAND USING ORDINARY KRIGING," *BAREKENG: J. Math. & App.*, vol. 19, no. 3, pp. 1791-1804, September, 2025.

Copyright © 2025 Author(s)

Journal homepage: <https://ojs3.unpatti.ac.id/index.php/barekeng/>

Journal e-mail: barekeng.math@yahoo.com; barekeng.journal@mail.unpatti.ac.id

Research Article · Open Access

1. INTRODUCTION

Indonesia is located between two continents, the Asian Continent and the Australian Continent, and between two oceans, the Indian Ocean and the Pacific Ocean [1]. Overall, Indonesia is at the center of a complex monsoonal system, where interactions between continents, oceans, and atmospheric and ocean dynamics play an essential role in determining weather and climate patterns. However, global warming has significantly impacted Indonesia's climate, including changes in temperature, rainfall patterns, sea level, and extreme weather events.

Global warming has caused changes in rainfall patterns in Indonesia. Runtunuwu's research found that there was a change in rainfall patterns in 128 years, from 1879 to 2007 [2]. In Java Island, this is evident from the two-month reduction in wet months. This resulted in a decrease in the planting period. In 2020, rain with an intensity above 200 mm/day was recorded in Jakarta and surrounding areas. At Halim Perdanakusuma Airport, the annual rain intensity of 377 mm/day was the highest since 1866 [3].

Java Island is still the center of economic, social, and cultural activities in Indonesia. Indonesia's economic growth in the first quarter of 2023 was still dominated by growth in Java, with a contribution of 57.17% [4]. Java Island often experiences significant variations in rainfall. Over the past 20 years, several regions in Java have experienced an increase in rainfall ranging from 40 to 120 mm. Additionally, many areas on the island have seen a rise in the frequency of extreme rainfall events. Urban areas, in particular, tend to experience more extreme rainfall compared to rural regions, highlighting the growing impact of changing weather patterns across Java [5]. This variability has a significant impact on key sectors such as agriculture, food security, and water resource management in the region [6], [7], [8]. The climate on Java Island is generally tropical, with significant rainfall and stable temperatures throughout the year. There are two seasons on the island: the wet season and the dry season. The wet season usually occurs between October and April, with the highest rainfall in January and February.

On the other hand, the dry season usually lasts from May to September, with the lowest rainfall occurring in July and August. The climate is warmer and more humid along the coast compared to the cooler and more humid mountainous regions [9]. With global climate change becoming more pronounced, a better understanding of the spatial distribution of rainfall is becoming increasingly important to anticipate its impact on society and the environment in Java.

Rainfall intensity information is vital in weather monitoring, disaster management, and planning in agriculture and development [10]. However, monitoring points often experience problems such as equipment damage or measurement errors. This can cause the data collected to be inaccurate or incomplete. Another problem is the limited number of rain intensity measuring instruments in remote areas. Not all locations in Java Island have observation stations. Therefore, it is necessary to analyze the prediction of rainfall intensity for areas where rainfall intensity data cannot be collected. The analysis can be done by utilizing the linkage and similarity of rainfall patterns between adjacent regions. Regarding geographical structure, there is a specific pattern in climate change where areas close to each other show similar weather characteristics. For example, Java Island, one of Indonesia's most populous regions, displays similar weather patterns despite significant local variations.

One approach to overcoming data gaps is leveraging the spatial relationships and similarities in rainfall patterns between adjacent regions. Regarding geographical structure, climate variations follow a specific pattern, where neighboring areas often exhibit similar weather characteristics. For example, despite its significant local variations, Java Island—one of the most populous regions in Indonesia—displays relatively consistent weather patterns. Understanding these spatial correlations enables more effective rainfall estimation.

The most fundamental method for spatial estimation is Inverse Distance Weighting (IDW), which predicts values at unknown locations based on their proximity to known observation points. IDW assigns higher weights to closer points, assuming that nearby locations have more similar rainfall patterns. However, a key limitation of IDW is that it does not account for spatial dependencies or variations beyond simple distance relationships, making it less reliable in complex geographic conditions.

A more advanced approach, Kriging, improves upon IDW by incorporating spatial autocorrelation through semivariogram modeling. A semivariogram quantifies the relationship between variability and distance among observed locations, allowing Kriging to produce more accurate predictions, particularly in regions with strong spatial dependence. Unlike IDW, which solely relies on distance-based weighting,

Kriging optimizes interpolation by considering statistical relationships between sampled data points. Given Java Island's diverse topography and microclimatic variations, Kriging is better suited for capturing spatial rainfall distributions, making it the preferred method for estimating rainfall intensity in unsampled locations.

The study on the implementation of Inverse Distance Weighting (IDW) and Kriging methods for analyzing humidity and temperature distribution patterns due to weather changes in the Bangka Islands, based on data from 2019 to 2021, produced the following results: The standard error (SE) prediction for temperature using IDW ranges from 0.223 to 0.331, while for relative humidity, it ranges from 0.506 to 0.751. In this case, the Kriging method is better than the IDW method [11].

Research comparing IDW and Kriging model accuracy in groundwater table mapping further supports these findings. The study found that the best interpolation model for the IDW method was obtained using power (p) with a value of 3, generating an RMSE of 3.23 with a validity of 40%. Meanwhile, the best interpolation model for the Kriging method was obtained using the Ordinary Kriging variant, which produced an RMSE of 2.98 with a validity of 50%. These results indicate that the Kriging method is more accurate than the IDW method, yielding a lower RMSE and higher validity [12]. Based on this background, the researcher intends to develop a Kriging equation to estimate rainfall intensity at unsampled points on Java Island using rainfall intensity values from sampled points, providing a more reliable and precise prediction model.

2. RESEARCH METHODS

2.1 Semivariogram

A variogram is a statistical tool used to describe autospatial modeling and exploration of regional variables, while a semivariogram is one-half of a variogram. Semivariograms are divided into two types, namely experimental semivariograms and theoretical semivariograms. The experimental semivariogram is obtained from the measurement of spatial data, and the experimental semivariogram formula can be seen in **Equation (1)** as follows [13].

$$\hat{\gamma}(h) = \frac{1}{N(h)} \sum_{i=1}^{N(h)} [Z(s_i) - Z(s_i + h)]^2 \quad (1)$$

where,

$\hat{\gamma}(h)$: semivariogram value at distance h .

$Z(s_i)$: value of observation at $i - th$ location.

$Z(s_i + h)$: the value of the observation at $i - th$ location with the addition of distance h .

$N(h)$: many pairs of data that have a distance h .

In the experimental semivariogram there are three parameters, namely:

- Sill (C) is the stable period in the semivariogram that has reached the range, where the Sill value is equal to the value of the variance.
- Nugget Effect (C_0) is a jump from a value of 0 to the semivariogram value with the smallest distance.
- Range (a) is the distance from the semivariogram to reach a stable state (sill).

The value of the experimental semivariogram is used for further analysis by replacing the experimental semivariogram with a theoretical semivariogram. There are three commonly used theoretical semivariogram models, as can be seen in **Equation (2)**, **Equation (3)**, and **Equation (4)**, as follows [14].

- Spherical Model

$$\gamma(h) = \begin{cases} c \left[\frac{3h}{2a} - \left(\frac{h}{2a} \right)^3 \right], & \text{for } h \leq a \\ c, & \text{for } h > a \end{cases} \quad (2)$$

b. Exponential Model

$$\gamma(h) = \begin{cases} c \left[1 - \exp\left(-\frac{h}{a}\right) \right], & \text{for } h \leq a \\ c, & \text{for } h > a \end{cases} \quad (3)$$

c. Gaussian Model

$$\gamma(h) = \begin{cases} c \left[1 - \exp\left(-\frac{h^2}{a^2}\right) \right], & \text{for } h \leq a \\ c, & \text{for } h > a \end{cases} \quad (4)$$

with,

h : sample location distance

c : sill

a : range

The following images of the three theoretical models are as follows:

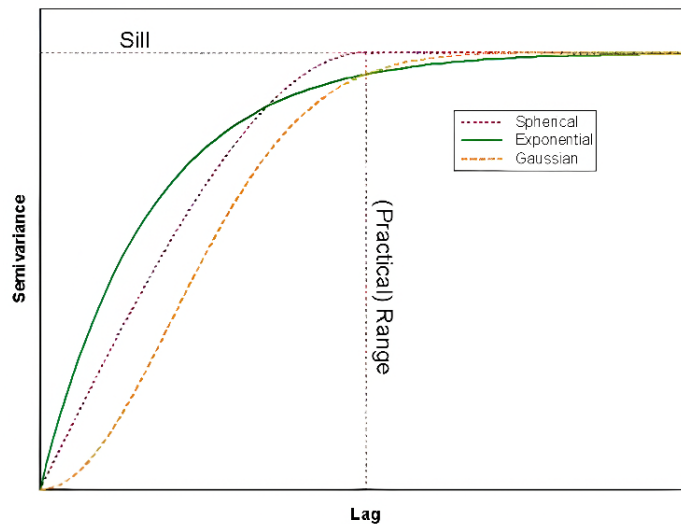


Figure 1. Comparison of Three Theoretical Models [15]

2.2 Kriging

The kriging method is a linear interpolation technique to predict values at unsampled locations based on realized values at surrounding locations. The kriging method consists of three methods, namely Simple Kriging (SK), Ordinary Kriging (OK), and Universal Kriging (UK). SK is used when the average is known, OK is used when the average is unknown and assumed to be constant, and UK is used when the average is unknown and not constant [16].

The OK method is used when the population mean is unknown and assumed to be constant. This assumption aligns with real-world data characteristics, where the actual population mean is often challenging to determine. In many practical cases, especially in geospatial data such as rainfall, the underlying mean is not explicitly known due to the heterogeneous and dynamic nature of spatial phenomena. Rainfall patterns, for instance, vary across regions and are influenced by multiple environmental factors, making it nearly impossible to define a single, known global mean. Therefore, assuming a locally constant but unknown mean, as done in Ordinary Kriging, provides a more realistic and flexible approach to spatial interpolation [17].

In Ordinary Kriging (OK), spatial dependence between locations can be represented using a covariance function or variogram as a distance function. However, this is valid only if the data satisfy second-order

stationarity. Second-order stationarity assumes that (1) the mean remains constant across the study domain and (2) the covariance between two locations depends only on the distance between them, not their absolute coordinates. The OK method consists of point OK and block OK, where the interpolation result with point OK is a point while the block OK interpolation result is an area around the interpolation point. This research is limited to the ordinary point kriging method [17].

2.3 Ordinary Point Kriging

The underlying model of point kriging and block kriging is the generalized OK equation model as can be seen in Equation (5) as follows.

$$Z(s) = \mu + \varepsilon(s) \quad (5)$$

where μ is assumed to be fixed and unknown while $\varepsilon(s)$ has a mean of zero, describing the variation around the mean. If there are n observations at a known location and we want to know the prediction \hat{Z} of Z at an unsampled location s_0 , 3 basic assumptions are required that ensure the prediction \hat{Z} can be obtained.

- \hat{Z} is linear on $Z(s_1), \dots, Z(s_n)$
- \hat{Z} is unbiased predictor
- \hat{Z} minimizes the mean square error of the prediction $E[Z(s_0) - \hat{Z}(s_0)]^2$

2.3.1 Linearity and Unbiasedness in Ordinary Point Kriging

Ordinary point kriging is the estimation of a value at a given point and is often used in spatial interpolation analysis in general. Suppose Z has a measure at the sample points s_i with $i = 1, 2, \dots, n$. The information from this sample is used to estimate the value at a certain unsampled point s_0 with Equation (6) as follows:

$$\hat{Z}(s_0) = \sum_{i=1}^n \lambda_i Z(s_i) \quad (6)$$

The equation is formed from the first assumption which states that \hat{Z} is linear in $Z(s_1), \dots, Z(s_n)$. In the equation, n represents the sample data points and λ_i represents the kriging weights. The second assumption states that is an unbiased estimator, so Equation (7) is obtained as follows [17].

$$\begin{aligned} E(Z^*(s_0) - Z(s_0)) &= E\left(\sum_{i=1}^n \lambda_i Z(s_i) - Z(s_0)\right) \\ &= \sum_{i=1}^n \lambda_i E(Z(s_i)) - E(Z(s_0)) \\ &= \mu \sum_{i=1}^n \lambda_i - \mu = 0 \Leftrightarrow \sum_{i=1}^n \lambda_i = 1 \end{aligned} \quad (7)$$

then it is obtained that the weights become unbiased with $\sum_{i=1}^n \lambda_i = 1$.

2.3.2 Minimum Variance on Ordinary Point Kriging

The minimum variance is obtained by minimizing the mean square value of the errors $E[(Z(s_0) - \hat{Z}(s_0))^2]$ [17]. To fulfill this condition, a linear constant λ_i and a lagrange multiplier m are required, which guarantees that the sum of the kriging weights will sum to 1 as shown in Equation (8) below.

$$L = E[(Z(s_0) - \hat{Z}(s_0))^2] - m\left(\sum_{i=1}^n \lambda_i - 1\right)$$

$$\begin{aligned}
 L &= E \left[\left(Z(s_0) - \sum_{i=1}^n \lambda_i Z(s_i) \right)^2 \right] - m \left(\sum_{i=1}^n \lambda_i - 1 \right) \\
 L &= \text{Var}(Z(s_0)) - 2 \sum_{i=1}^n \lambda_i \text{Cov}(Z(s_0), Z(s_i)) + \sum_{i=1}^n \sum_{j=1}^n \lambda_i \lambda_j \text{Cov}(Z(s_i), Z(s_j)) \\
 &\quad - m \left(\sum_{i=1}^n \lambda_i - 1 \right)
 \end{aligned} \tag{8}$$

By performing partial derivatives of equation L on λ_i and α which are then equated to zero. This will result in the following system of **Equation (9)**.

$$\text{Cov}(Z(s_0), Z(s_i)) = \sum_{j=1}^n \lambda_j \text{Cov}(Z(s_i), Z(s_j)) - \alpha, \quad \text{for } i = 1, 2, \dots, n \tag{9}$$

by $\sum_{i=1}^n \lambda_i = 1$.

Based on the above system, we get $\sum_{j=1}^n \lambda_j \text{Cov}(Z(s_i), Z(s_j)) = \text{Cov}(Z(s_0), Z(s_i)) + \alpha$, so the minimum variance prediction under the condition of unbiasedness is as in **Equation (10)** below:

$$\begin{aligned}
 \sigma_{OK}^2 &= \text{Var}(Z(s_0)) - 2 \sum_{i=1}^n \lambda_i \text{Cov}(Z(s_0), Z(s_i)) + \sum_{i=1}^n \lambda_i \text{Cov}(Z(s_0), Z(s_i)) + \alpha \\
 \sigma_{OK}^2 &= \text{Var}(Z(s_0)) - \sum_{i=1}^n \lambda_i \text{Cov}(Z(s_0), Z(s_i)) + \alpha
 \end{aligned} \tag{10}$$

However, unknown values are still required to estimate the covariance function. The sample mean value estimates the covariogram. The covariogram is estimated by the sample mean value. However, in the case of spatial dependence, the covariogram generated from the sample is an unbiased estimator and is not of minimum variance. An alternative solution is to use other mean values that account for spatial dependencies. One of them is using semivariograms in the OK equation system, as in the following **Equation (11)** system [17].

$$\gamma(s_i, s_0) = \sum_{j=1}^n \lambda_j \gamma(s_i, s_j) + \alpha, \quad \text{for } i = 1, 2, \dots, n \tag{11}$$

by $\sum_{i=1}^n \lambda_i = 1$.

2.3.3 Estimation on Ordinary Point Kriging

The weight vector and lagrange multiplier can be formed from the covariance matrix or semivariogram. The optimal kriging weights can be obtained with the semivariogram matrix through **Equation (12)** below.

$$\Gamma \lambda = \Gamma_0 \tag{12}$$

Where A is the semivariogram matrix between the sample data points, A_0 is the semivariogram vector between the sample data points and the target, and λ is the weight vector of kriging and lagrange multiplier. The system of equations can be written in matrix form as in **Equation (13)** as follows:

$$\begin{pmatrix} \gamma_{11} & \gamma_{12} & \gamma_{13} & \dots & \gamma_{1n} & 1 \\ \gamma_{21} & \gamma_{22} & \gamma_{23} & \dots & \gamma_{2n} & 1 \\ \gamma_{31} & \gamma_{32} & \gamma_{33} & \dots & \gamma_{3n} & 1 \\ \vdots & \vdots & \vdots & \ddots & \vdots & \vdots \\ \gamma_{n1} & \gamma_{n2} & \gamma_{n3} & \dots & \gamma_{nn} & 1 \\ 1 & 1 & 1 & \dots & 1 & 0 \end{pmatrix} \begin{pmatrix} \lambda_1 \\ \lambda_2 \\ \lambda_3 \\ \vdots \\ \lambda_n \\ \mu \end{pmatrix} = \begin{pmatrix} \gamma_{10} \\ \gamma_{20} \\ \gamma_{30} \\ \vdots \\ \gamma_{n0} \\ 1 \end{pmatrix} \quad (13)$$

Furthermore, to get the solution of the kriging weight value and Lagrange multiplier, the following **Equation (14)** is used:

$$\lambda = \Gamma^{-1}\Gamma_0 \quad (14)$$

2.3.4 Analysis Steps Using the Ordinary Point Kriging Method

- a. The spatial data location map used is the map digitized in the preparation stage. The digitized map contains spatial data attribute information.
- b. Identifying the fulfillment of spatial data assumptions, including the assumptions of normality, spatial variance homogeneity, and spatial autocorrelation.
 - i. The assumption of normality was tested using the Kolmogorov Smirnov test.
 - ii. The assumption of homogeneity of spatial data variance uses data plotting against altitude and longitude. Based on the general kriging model, which is as in **Equation (15)** below:

$$Z(s) = \mu + e(s), \quad e(s) \in D \subset R^2 \quad (15)$$

Then the error variance of a constant (homogeneous) model is obtained as **Equation (16)** below:

$$\begin{aligned} V(\varepsilon_i) &= E(\varepsilon_i - E(\varepsilon))^2 \\ V(\varepsilon_i) &= E(\varepsilon_i)^2 \\ V(\varepsilon_i) &= \sigma^2 \end{aligned} \quad (16)$$

The tendency of the plot between spatial data and longitude indicates that there is a trend according to the increase in longitude, and also applies to latitude.

- iii. The assumption of spatial autocorrelation is performed using a descriptive variogram.
- c. Form various empirical semivariogram models, then select the model that produces the best kriging spatial interpolation based on the RMSE and MAE values.
- d. Using the Ordinary Point Kriging interpolation method to determine the prediction contour map at each point on the map using **Equation (17)** as follows:

$$\hat{Z}(s_0) = \sum_{i=1}^n \lambda_i Z(s_i) \text{ and } \hat{Z}(s_0) = \lambda_1 Z(s_1) + \lambda_2 Z(s_2) + \dots + \lambda_n Z(s_n) \quad (17)$$

- e. Using the Ordinary Point Kriging interpolation method to determine the prediction standard error contour map at each point on the map based on the root of **Equation (18)** below:

$$\sigma^2 = (s_0) = C(0) - \sum_{i=1}^n \lambda_i \gamma(s_i, s_0) + m \quad (18)$$

where $C(0) = C_0 + C_1 = \sigma^2$ and m represents the Lagrange multiplier which calculated to ensure that the Ordinary Kriging estimation is unbiased.

- f. Calculate the RMSE and MAPE values for the Ordinary Point Kriging method with **Equation (19)** and **Equation (20)** as follows:

$$\text{RMSE} = \sqrt{\frac{1}{n} \sum_{i=1}^n [Z(s_i) - \hat{Z}(s_i)]^2} \quad (19)$$

where, $Z(s_i)$ is the true value of the data at the $i - th$ location, $\hat{Z}(s_i)$ is the expected value of the data at the $i - th$ location and n is the amount of research data.

$$\text{MAPE} = \frac{1}{n} \sum_{i=1}^n \left| \frac{Z(s_i) - \hat{Z}(s_i)}{Z(s_i)} \right| \times 100\% \quad (20)$$

A good estimation accuracy for the kriging method is a low RMSE value and a small MAPE value. MAPE values are categorized into the following groups [18].

Table 1. MAPE Categorization

MAPE	Description
$\leq 10\%$	Highly Accurate
10 - 20%	Accurate
20 - 50%	Reasonable
$> 50\%$	Inaccurate

3. RESULTS AND DISCUSSION

3.1 Descriptive Statistics

The data used in this study is the average rainfall data in the Java Island region within 10 years (2013 to 2023) obtained from the NASA POWER website <https://power.larc.nasa.gov/data-access-viewer/>. The data used consists of 64 observation locations in the Regency / City area on the island of Java [19], as shown in **Figure 2**. In this study, the data is divided into two groups, namely training and test data. Training data is data included in the formation of kriging equations, while test data is used to test the accuracy of kriging models in predicting unsampled areas. The training data consists of 53 regions, while the test data consists of eleven regions. In **Figure 2**, the blue dots represent training data locations, while the black dots indicate testing data points used to evaluate the kriging model.

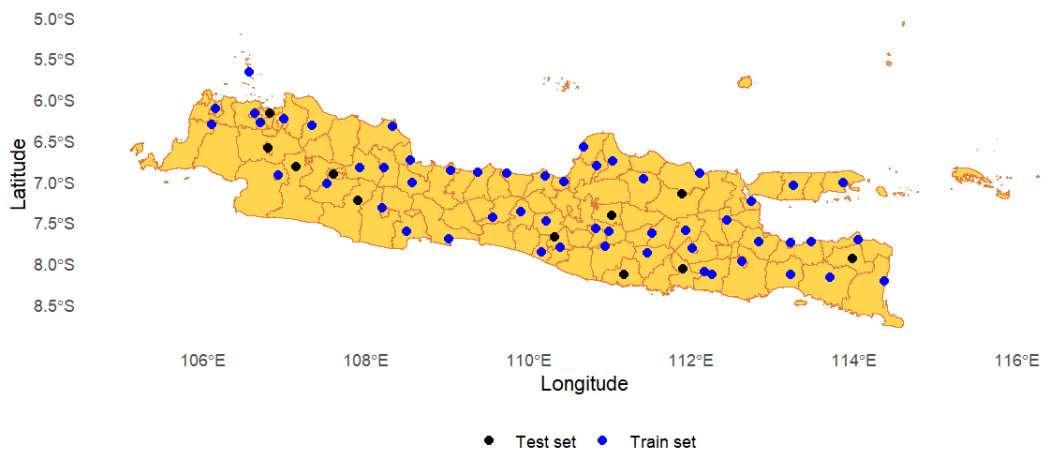


Figure 2. Distribution of Meteorological Observation Stations Across Java

From the training data, it was found that the minimum value of rainfall was 167.2 mm/day at Sumenep Regency, while the maximum value reached 333 mm/day at Tasikmalaya Regency. This data has a median

data centering measure of 199.3 mm/day and an average of 208.6 mm/day. The data distribution was measured using standard deviation and variance with values of 31.7 mm/day and 1003.6 mm/day respectively. The rainfall data from this training data group has a non-symmetrical data distribution, as seen in **Figure 3**.

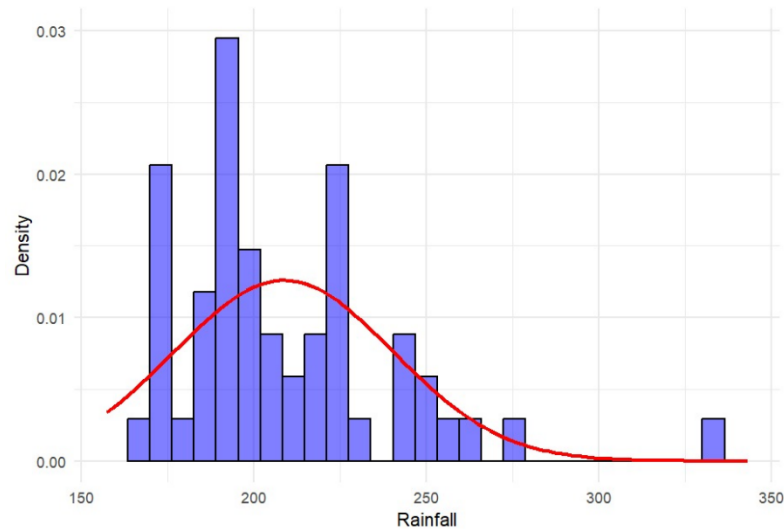


Figure 3. Histogram of Training Data

The histogram displays the frequency distribution of rainfall data, with most values concentrated around 200 mm, while higher rainfall values occur less frequently, indicating a right-skewed distribution. The red density curve represents a smoothed probability distribution, highlighting the overall trend. This visualization helps understand rainfall patterns, identify anomalies, and support further climatological analysis.

3.2 Normality Test and Data Transformation

The normality test is carried out to determine whether the data is normally distributed. The test is carried out using the Kolmogorov-Smirnov test, which calculates the absolute difference between the cumulative frequency distribution and the standard normal distribution. The hypothesis in the Kolmogorov-Smirnov test is as follows:

H_0 : Logarithmic transformed rainfall data follows a normal distribution.

H_1 : Logarithmic transformed rainfall data does not follow a normal distribution.

The following are the normality test results on the data after logarithmic transformation.

Table 2. Normality Test Results Using the Kolmogorov-Smirnov Test

D	p-value	Decision
0.12327	0.04318	H_0 failed rejected

Based on the results in **Table 2**, using a significance level of 1%, it can be concluded that the null hypothesis fails to be rejected, which means that the data in this study have followed a normal distribution.

3.3 Data Distribution

Ordinary kriging requires assuming the data is second-order stationary [20]. One way to check the stationarity of the data is through data visualization. The data resulting from the logarithmic transformation of rainfall values will then be plotted against regional coordinates (latitude and longitude) to see if there is a tendency to change rainfall values when latitude and longitude coordinate values occur.

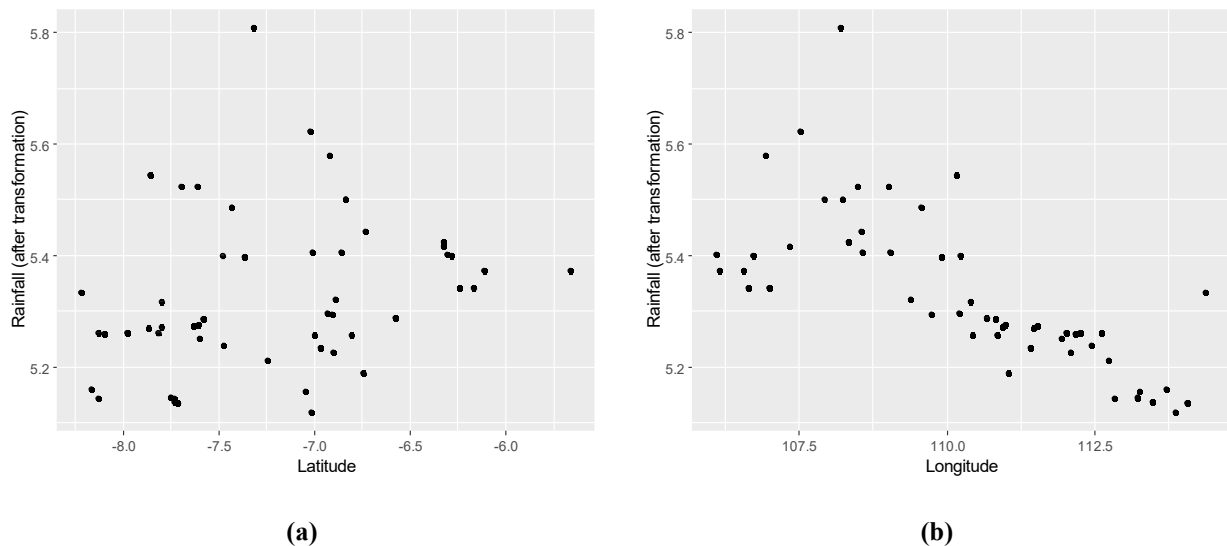


Figure 4. Scatter Plot of Inflation Values Based on Coordinates of Districts/Cities in Sampled Region (a) Latitude (b) Longitude

Figure 4 (a) shows no particular trend or pattern in the plot between the transformed data and latitude. However, the plot shows a downward trend between the transformed data and longitude, as shown in **Figure 4** (b). It indicates a relationship between the transformed rainfall variables and changes in longitude. In this case, changes in rainfall occur along with changes in longitude. The higher the longitude of an area (for example, East Java), the more the average rainfall tends to decrease. If there is a specific pattern in any of the plots, it is not enough to conclude that the average rainfall data is stationary. If the data of the sampled region satisfies the second-order stationary condition, the ordinary kriging system can be expressed in terms of a semivariogram [17].

3.4 Semivariogram

The semivariogram is calculated between two points of the observation region, so out of 53 sampled regions, there will be $C(53,2)$ or 1378 sample pairs. The experimental semivariogram value can be calculated using the equation mentioned in the previous chapter, specifically in **Equation (1)**. With the help of the R programming language, using gstat package, the experimental semivariogram plot is obtained, as shown in **Figure 5**.

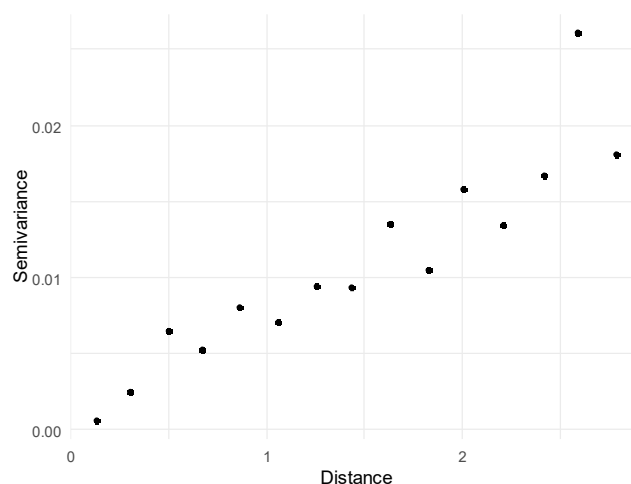
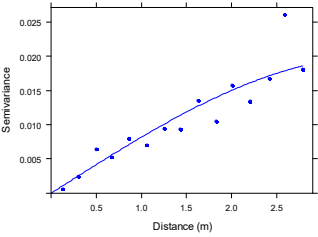
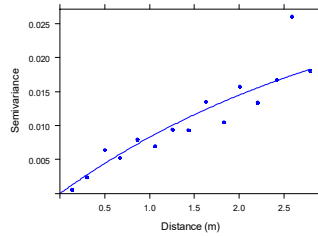
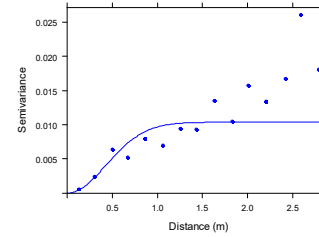


Figure 5. Experimental Semivariogram Plot

Next, we will look for the theoretical semivariogram that best matches the experimental semivariogram that has been obtained. In calculating the theoretical semivariogram, the sill parameter is required. The sill value can be obtained from the variance of the sampled data. The most suitable theoretical model is determined based on the smallest sum squared error (SSE) value.

This study uses three theoretical semivariogram models: the spherical, exponential, and Gaussian. Based on the calculation, the value of a sill obtained is 0.02009, which will be used in theoretical modeling. **Table 3** compares each theoretical model's plot, sill value, range, and SSE. Based on these results, the exponential model is the most suitable because it has the smallest SSE value.

Table 3. Comparison of Theoretical Semivariograms

	Spherical	Exponential	gaussian
psill	0.0198	0.0331	0.0103
range	3.5412	3.4849	0.6069
SSE	0.002194	0.002015	0.004746
plot			

3.5 Control Location Prediction Results

After obtaining the best theoretical semivariogram model, the following prediction of rainfall data at the control location is based on the exponential theoretical semivariogram model. Based on **Table 4**, it can be seen that the predicted rainfall results in 11 districts/cities, which are the control locations using the ordinary point kriging method, are close to the results of the actual data. Next, the average percentage value of the residual between the predicted data and the actual data (MAPE) will be used to measure the accuracy of the prediction results.

The MAPE value obtained is 4.845%. The MAPE value <10% indicates a very accurate prediction accuracy level [18], showing that rainfall prediction with the ordinary point kriging method can be applied in districts/cities on the island of Java that are not sampled.

Table 4. Rainfall Prediction Results and MAPE Values at the Control Site

Number	Regency/City	Actual Data	Prediction Result	MAPE
1	Bondowoso Regency	174.2182	176.9082	4.84541%
2	Bojonegoro Regency	186.1631	188.5542	
3	Tulungagung Regency	192.6200	194.1086	
4	Pacitan Regency	194.1487	199.2501	
5	Sragen Regency	195.2403	193.4561	
6	Sleman Regency	197.5060	215.4605	
7	Central Jakarta City	209.0427	211.4250	
8	Bogor City	221.5168	237.6515	
9	Garut Regency	245.1586	298.1771	
10	Cianjur Regency	265.0026	257.5753	
11	Bandung City	276.6233	264.9668	

The results of this study demonstrate the applicability and accuracy of the ordinary point kriging method for predicting rainfall at unsampled locations in Java. The low MAPE value of 4.845% signifies that the method provides highly accurate predictions, as supported by the criterion that MAPE values below 10% indicate a strong level of accuracy [18]. These results are likely influenced by the choice of semivariogram function and the complexity of the model used. Ordinary point kriging adopts a more straightforward approach, focusing on spatial relationships between points. This simplicity enables the model to produce more stable interpolations and better generalization, as evidenced by the lower MAPE value in this study. It is also important to highlight that overly simplistic interpolation methods, such as Inverse Distance Weighting (IDW), are often less accurate in predicting environmental data. IDW assumes that data influence depends

solely on distance without accounting for more complex spatial patterns, leading to biased results in areas with uneven data distribution [12], [13].

4. CONCLUSIONS

Using the ordinary point kriging method to predict rainfall on Java Island has proven effective. The resulting kriging equation provides rainfall predictions with a high level of accuracy, indicated by a MAPE value of 4.85% and an RMSE of 18.17. This research can enrich the understanding of climate patterns in Java Island and contribute to developing mitigation and adaptation strategies for climate change in Indonesia. These results show that utilizing spatial dependencies can be a helpful approach to predicting rainfall variability in climatically complex regions such as Indonesia.

ACKNOWLEDGMENT

The authors would like to thank the Rector of Universitas Padjadjaran, Director of DRPM Universitas Padjadjaran, Center for Modeling and Computation Studies FMIPA Universitas Padjadjaran for providing research funds for the dissemination of research results of lecturers and students through the Academic Leadership Grant with contract number: 1425/UN6.3.1/PT.00/2024.

REFERENCES

- [1] A. Noviyani, T. Nopsopon, and K. Pongpirul, "VARIATION OF TUBERCULOSIS PREVALENCE ACROSS DIAGNOSTIC APPROACHES AND GEOGRAPHICAL AREAS OF INDONESIA," *PLoS One*, vol. 16, no. 10 October, Oct. 2021. doi: <https://doi.org/10.1371/journal.pone.0258809>
- [2] E. Runtuuwu and D. H. Syahbuddin, "PERUBAHAN POLA CURAH HUJAN DAN DAMPAKNYA TERHADAP PERIODE MASA TANAM," 2007.
- [3] A. Arif, "PERUBAHAN POLA HUJAN DI JAKARTA DALAM SEABAD DAN IMPLIKASINYA," *kompas.id*. Accessed: April 21, 2024. [Online]. Available at: <https://www.kompas.id/baca/ilmu-pengetahuan-teknologi/2022/04/18/perubahan-pola-hujan-di-jakarta-dalam-seabad-dan-implikasinya>.
- [4] CNN Indonesia, "BPS: PEREKONOMIAN INDONESIA MASIH TERPUSAT DI PULAU JAWA," *CNN Indonesia*, 05-05-2023. Accessed: May 24, 2024. [Online]. Available at: <https://www.cnnindonesia.com/ekonomi/20230505113652-532-945647/bps-perekonomian-indonesia-masih-terpusat-di-pulau-jawa>.
- [5] Universitas Gadjah Mada, "BANYAK FAKTOR PENGARUHI TINGGINYA CURAH HUJAN," *Universitas Gadjah Mada*, 20-Apr-2022. [Online]. Available: <https://ugm.ac.id/id/berita/22459-pengamat-ugm-banyak-faktor-pengaruh-tingginya-curah-hujan/>. [Accessed: 30-Mar-2025].
- [6] A. B. Sekaranom, E. Nurjani, and F. Nucifera, "AGRICULTURAL CLIMATE CHANGE ADAPTATION IN KEBUMEN, CENTRAL JAVA, INDONESIA," *Sustainability (Switzerland)*, vol. 13, no. 13, Jun. 2021. doi: <https://doi.org/10.3390/su13137069>
- [7] R. Rahayu, S. A. Mathias, S. Reaney, G. Vesuviano, R. Suwarman, and A. M. Ramdhan, "IMPACT OF LAND COVER, RAINFALL AND TOPOGRAPHY ON FLOOD RISK IN WEST JAVA," *Natural Hazards*, vol. 116, no. 2, pp. 1735–1758, Mar. 2023. doi: <https://doi.org/10.1007/s11069-022-05737-6>
- [8] B. D. A. Nugroho, C. Arif, F. Suryandika, H. N. Annisa, and S. I. Wijayanti, "RELATIONSHIPS AMONG GLOBAL CLIMATE INDICES, RAINFALL PATTERNS, AND CROP PRODUCTIVITY IN THE SOUTHERN PART OF JAVA, INDONESIA," *Ecological Engineering & Environmental Technology*, vol. 25, no. 10, pp. 87–95, Oct. 2024. doi: <https://doi.org/10.12912/27197050/191332>
- [9] M. Harris, "BATAS LAUT PULAU JAWA," Accessed: April 21, 2024. [Online]. Available at: <https://www.gamedia.com/literasi/batas-laut-pulau-jawa/>.
- [10] H. Chandra and H. Suprpto, "SISTEM INFORMASI INTENSITAS CURAH HUJAN DI DAERAH CILIWUNG HULU," *Jurnal Informatika dan Komputer*, vol. 21, no. 3, 2016.
- [11] R. Amelia, E. Julianti, and Guskarnali, "IMPLEMENTATION OF INVERSE DISTANCE WEIGHTING (IDW) AND KRIGING METHOD FOR DISTRIBUTION PATTERN HUMIDITY AND TEMPERATURE DATA ON WEATHER CHANGES IN THE BANGKA ISLANDS," in *IOP Conference Series: Earth and Environmental Science*, Institute of Physics, 2023. doi: <https://doi.org/10.1088/1755-1315/1267/1/012091>
- [12] S. P. Sejati, "PERBANDINGAN AKURASI METODE IDW DAN KRIGING DALAM PEMETAAN MUKA AIR TANAH," *Majalah Geografi Indonesia*, 2019.
- [13] G. Chen, Y. Yang, X. Liu, and M. Wang, "SPATIAL DISTRIBUTION CHARACTERISTICS OF HEAVY METALS IN SURFACE SOIL OF XILINGUOLE COAL MINING AREA BASED ON SEMIVARIOGRAM," *ISPRS Int J Geoinf*, vol. 10, no. 5, May 2021. doi: <https://doi.org/10.3390/ijgi10050290>
- [14] E. H. Isaaks and R. M. Srivastava, "APPLIED GEOSTATISTICS," 1989.

- [15] A. N. Falah *et al.*, “AN EXPANDED SPATIAL DURBIN MODEL WITH ORDINARY KRIGING OF UNOBSERVED BIG CLIMATE DATA,” *Mathematics*, vol. 12, no. 16, Aug. 2024. doi: <https://doi.org/10.3390/math12162447>
- [16] E. Ashrafpour, “DIFFERENCE BETWEEN SIMPLE KRIGING AND ORDINARY KRIGING,” Mar. 2021.
- [17] J.-M. Montero, G. Fernández-Avilés, and J. Mateu, *SPATIAL AND SPATIO-TEMPORAL GEOSTATISTICAL MODELING AND KRIGING*, 1st ed. Wiley, 2015.
- [18] S. Salsabilla, A. F. Syaharni, and N. Chamidah, “ENTHUSIASTIC INTERNATIONAL JOURNAL OF APPLIED STATISTICS AND DATA SCIENCE PREDICTION OF PM2.5 IN DKI JAKARTA USING ORDINARY KRIGING METHOD,” *Enthusiastic International Journal of Applied Statistics and Data Science*, vol. 3, no. 1, pp. 48–58, 2023. doi: <https://doi.org/10.20885/enthusiastic.vol3.iss1.art5>
- [19] A. N. Falah, “SPATIAL AUTOREGRESSIVE EXOGENOUS KRIGING CLUSTERING MODEL AND ITS APPLICATION TO CLIMATE DATA IN INDONESIA,” Padjadjaran University, 2024.
- [20] D. A. Lubis and S. Fauziah, “METODE ORDINARY POINT KRIGING UNTUK MEMPREDIKSI INFLASI DI KABUPATEN/ KOTA YANG TIDAK TERSAMPEL,” *Jurnal Litbang Sukowati*, vol. 2, pp. 36–48, 2018. doi: <https://doi.org/10.32630/sukowati.v2i1.41>

